

Research Article

Identification of Variations in the Climatic Conditions of the Lerma-Chapala-Santiago Watershed by Comparative Analysis of Time Series

Luis Ricardo Manzano-Solís ¹, Miguel A. Gómez-Albores ², Carlos Díaz-Delgado ²,
Carlos Alberto Mastachi-Loza,² Raymundo Ordoñez-Sierra,² Khalidou M. Bâ ²
and Roberto Franco-Plata¹

¹Facultad de Geografía, Universidad Autónoma del Estado de México, Toluca, MEX, Mexico

²Centro Interamericano de Recursos del Agua, Facultad de Ingeniería, Universidad Autónoma del Estado de México, Toluca, MEX, Mexico

Correspondence should be addressed to Miguel A. Gómez-Albores; magomeza@uaemex.mx

Received 14 December 2017; Accepted 10 April 2018; Published 9 May 2018

Academic Editor: Enrico Ferrero

Copyright © 2018 Luis Ricardo Manzano-Solís et al. This is an open access article distributed under the Creative Commons Attribution License, which permits unrestricted use, distribution, and reproduction in any medium, provided the original work is properly cited.

The current study presents a method for automating the Köppen–García climate classification using a GIS module. This method was then applied in a case study of the Lerma-Chapala-Santiago watershed to compare time series data on climate from 1960 to 1989, 1981 to 2010, and 1960 to 2010. The kappa statistic indicated that the climate classifications of the generated model had a perfect degree of agreement with those of a prior nonautomated study. The climate data from the period 1960 to 2010 were used to create a climate map for the watershed. Overall, the dominant climates were dry, semiarid, temperate, and semiwarm temperate with a summer rainfall pattern. A comparative analysis of climate behavior between 1960 and 1989 and between 1981 and 2010 showed changes in temperature and extreme temperatures over 13.6% and 9.9%, respectively, of the watershed; the presence or absence of mid-summer drought also changed over 0.8% of the watershed. The module developed herein can be used to classify climates across all of Mexico, and data of varying spatial resolution and coverage can be inputted to the module. Finally, this module can be used to automate the creation of climate maps or to update climate maps at diverse spatial-temporal scales.

1. Introduction

Climate variations fundamentally influence human culture, society, and productive activities worldwide. The study and understanding of climate patterns are necessary for making decisions concerning human welfare. For example, climate is taken into consideration during the design of housing projects or during the estimation of costs for the hydraulic infrastructure. In addition, human society currently faces several complex issues regarding climate change, including how to adapt to and mitigate climate variability and change.

Climate changes are often associated with the deterioration of different human and natural systems. Alterations to climate stemming from human activities have resulted in more intense heat waves, droughts, flooding, tropical

cyclones, and forest fires. In addition, such alterations have disrupted food systems and water supplies and have frequently damaged the infrastructure. Also, under a changing climate, the output of climate-sensitive crops such as corn and wheat could potentially diminish, affecting production levels worldwide and threatening food security. Climate changes are also likely to lead to higher human mortality and morbidity as a result of increasing occurrence of infectious diseases (gastrointestinal, bronchial respiratory, and vector diseases). For these reasons, climate changes are important to study and monitor [1–4].

Diverse classification methods are available for characterizing climate. These methods have been applied with distinct objectives. Among the available methods and examples of their application, several studies may be

highlighted. For example, some studies have identified regions with greater agricultural productivity based on climate [5, 6]. Other studies have highlighted the effects of urbanization on microclimate [4, 7, 8]. Several additional studies have considered climate to improve housing design [9, 10]. Finally, the Köppen method is one proposal for classifying climate; this method was subsequently refined to improve its applicability across distinct landmasses and to therefore improve the accuracy of future climate studies [11].

The Köppen climate classification was adapted to Mexican climatic conditions by the Mexican researcher Enriqueta Garcia in the 1970s to better represent the diverse climate conditions of the country [12, 13]. This modified Köppen–Garcia method has been widely used by biologists, geographers, and agronomists in Mexico and throughout Central and South America from its conception to the present [14].

A review of recent literature confirms the continuing validity of the Köppen–Garcia classification system. For example, this classification system was employed in the “*Atlas of Climate Change Scenarios in the Yucatan Peninsula*” [15], in the analysis of possible climate change scenarios in the central zone of Veracruz [16], in the elaboration of a regional climate map for the 2011 Territorial and Ecological Land-Use Plan of the State of Durango, Mexico [17], and in the creation of a climate classification map for the Bahía de Banderas region of Mexico [18]. In addition, based on this classification system, the federal government of Mexico created an *Online Atlas* that displays a climate map for the country [19], and the National Institute of Statistics and Geography (INEGI, for its initials in Spanish) [20] generates, among other products, an official set of maps for Mexico that display various climatic and weather conditions nationwide at scales of 1 : 250,000, 1 : 500,000, and 1 : 1,000,000.

The rapid development of informatics in the last third of the previous century led to the development of numerous proposals to carry out the procedures of climate classification systems within computational environments. For example, Fuentes and Víctor [21] developed a spreadsheet in Microsoft Excel to classify climate based on data from meteorological stations following the Köppen–Garcia system. In addition, Sparovek et al. [22] developed a program in Microsoft Visual Basic to automate the Köppen climate classification for Brazil. Liu et al. [23] used Visual Basic 6.0 within a geographic information system (GIS) platform to project and interpolate climate based on available climate data and to subsequently display the resulting climate maps; in this method, data from numerous climate and agricultural indexes can be used. Ahmed [24] used Java to develop an educational Android application that uses Voronoi diagrams to generate climate zone maps according to the classification methods of Whittaker’s diagram, Köppen–Geiger, and the Holdridge life zones. An online map server was created by the Institute of Veterinary Public Health at the University of Veterinary Medicine, Vienna, Austria [25], to disseminate numerous climate maps from 1901 to 2100, based on the Köppen–Geiger climate classifications [26].

Despite the application of a wide variety of climate classifications in Mexico and the available set of tools for

carrying out such classifications, a GIS module for automatically performing the Köppen–Garcia climate classification is lacking. Specifically, the present study proposes the development of a GIS module for classifying climate based on raster layers of monthly rainfall and temperature data. This module then generates a resulting layer that displays the spatial behavior of different climate classes, thereby providing an overview of the climate types across a desired region of study. Moreover, this module can be used to study climate variability in space and time and can represent one application for the wide range of climate data collected by the Mexican National Meteorological Service (SMN, for its initials in Spanish) [27]. Finally, in Mexico, climate studies are currently necessary to create and update climate maps for different regions of the country at distinct territorial scales.

Based on the aforementioned context, the objectives of the current study are centered on developing an automated GIS module that could (a) carry out the procedures of the Köppen–Garcia climate classification, (b) determine climate classifications at the raster cell level within a GIS environment, (c) generate thematic maps with up-to-date meteorological data at any spatial scale in Mexico, (d) be simple and easy to use, (e) reduce execution time, and (f) process the large volumes of climate data that are currently available for Mexico. The functioning of the module was validated by applying the module to a case study of climate variations over time in the Lerma–Chapala–Santiago watershed.

2. Conceptual Framework

2.1. Climate and Its Classification. The Earth’s climate is determined by complex interactions between the sun, oceans, atmosphere, cryosphere, biosphere, and terrestrial surface. The sun is the main force that influences temperature and climate, yet its influence is unequally distributed across the Earth’s surface because of the Earth’s tilted rotation axis [28, 29]. In fact, climate stems from the Greek word *klima*, which means “inclination” [30]. According to the Intergovernmental Panel on Climate Change [29] and the World Meteorological Organization [31], climate is defined as the mean atmospheric temperature, the mean conditions of and/or variations in meteorological parameters (for a minimum of 30 years), or as the variations in the quantifiable measurements of these parameters. Under these definitions, climate is mainly determined by rainfall and temperature.

To reduce the complexity involved in studying different natural phenomena over large territorial scales, humans have often created simplified models that are more easily understood, managed, and reproduced. Similarly, climate classifications are one means of simplifying the large spatial and temporal variability in temperature and rainfall across the Earth’s surface by means of grouping regions with similar conditions or differentiating regions with respect to others.

During the last several centuries, diverse climate classifications have been developed. Several renowned systems include those developed by George Hadley in 1735, Wladimir Köppen in 1900, and Wladimir Köppen and Rudolf

Geiger in 1954, which resulted in the updated Köppen system. In 1948, C.W. Thornthwaite established a climate classification based on evapotranspiration. In 1968, Arthur Strahler proposed an additional classification [32] related to the main air masses across the planet. However, the first quantitative classification of world climate was presented by the scientist Wladimir Köppen in 1900. His work as a plant physiologist led him to realize that plants are indicators of climate conditions. Accordingly, he proposed five climate groups based on the vegetation groups previously determined by the French botanist Agustin Pyrame de Candolle: (a) equatorial climates, (b) arid climates, (c) warm temperate climates, (d) snow climates, and (e) polar climates [33]. Later, Rudolf Geiger collaborated with Köppen on his climate classification research, resulting in the Köppen–Geiger classification system, which was presented by Geiger in 1961; currently, this system is one of the most utilized around the world.

2.2. Adaption of the Köppen Climate Classification to Mexico. García [12] adapted the Köppen climate classification system to Mexico to create suitable classifications for the unique climatic conditions associated with the distribution of different plant formations in the country. The proposal for the original climate classification system used the latitudinal position of meteorological stations as the main determinant of climatic zones rather than considering variations in temperature and rainfall that are influenced by altitude or the presence of mountain ranges. However, in Mexico and other regions, variations in altitude create specific climate conditions.

Furthermore, the plant formations that corresponded with the latitudinally determined Köppen climate zones [12] were not applicable for Mexico, as the expected vegetation based on climate classifications and the actual observed vegetation frequently did not coincide. For example, “savannah climate” under the Köppen designation corresponds to what García [12] terms as “warm, subhumid climate with summer rains.” However, in Mexico, the thermal and humidity conditions that are associated with this classification are characteristic of high or low seasonal rain forests rather than savannah. In addition, the “steppe climates” of the Köppen classification adequately represent regions of Russia; however, in Mexico, this climate type is associated with cacti and thorny scrubland and is denominated by García [12] as “dry or arid climate.” A final example is the case of Köppen’s “tundra climates” [12], which García [12] labels as “cold climates.” This latter climate characterizes the elevated regions within the tropical zones of Mexico.

In the first step of the Köppen–García climate classification system [12], the main climate group (warm, temperate, dry, or cold) is determined based on temperature and humidity conditions. For this determination, data on average annual and monthly temperatures and on total annual and monthly rainfall are required. Then, the climate subgroup (semiwarm, semicold, cold, or very cold) is identified based on average annual and monthly temperatures. Specifically, the degree of humidity (humid, subhumid,

semiarid, arid, or very arid) and the rainfall pattern (summer, intermediate, or winter), which are determined from monthly and annual temperatures and rainfall, are used to establish the climate type and subtype. Additional descriptive conditions can be included, such as the presence of warm/cool or long/short summers. Finally, symbols are used to designate variants of the classifications and to express, for example, the presence of mid-summer drought, the degree of temperature variation (isothermal, low, extreme, or very extreme), and/or the annual course of temperature (to identify the presence of a Ganges-type temperature regime).

One of the issues surrounding climate classification is that classifications are generally based on the average daily, monthly, or annual values of climatic data collected from meteorological stations. However, temperature and rainfall occur continuously across a territory and are distributed rather than isolated events that vary across the Earth’s surface. Therefore, one complexity in the study of climate behavior stems from the measurement and recording of climatic variables as point data at conventional or automatic meteorological stations [27], as the existent network of stations is often unable to cover all locations within a study area. Spatially, this leads to significant discontinuities in climatic data.

Therefore, different methods have been developed to estimate climate parameters in areas where climatic data cannot be directly measured and to subsequently generate visual representations or images over a continuous area [34]. The process wherein values are estimated for areas between sampling points is called interpolation [34]. Several interpolation methods are available. Boer et al. [35] compared the interpolation methods of Kriging, co-Kriging, inverse distance weighting, and thin-plate smoothing spline for rainfall and temperature data and found that the thin-plate smoothing spline method provided the best results using the root mean squared error of prediction as the validation criterion. These procedures are a basic tool of climate analysis and have been integrated in computer programs, GIS environments, and other corresponding technologies, with the exception of the thin-plate smoothing spline method.

Despite these methods for spatially capturing and representing meteorological data, some authors [36] express concerns over the sufficiency and adequacy of networks of meteorological stations, as well as the successive interpolation of resulting meteorological data. Specifically, the coverage and adequacy of meteorological stations influence the accuracy of spatial layers generated from meteorological data. However, an evaluation of the conditions of the meteorological network remained outside the scope of the present paper.

Additionally, some existing computational and GIS software, both free and commercial, allows users to implement additional modules developed by other users. This is one advantage of the application program interface (API) of the GIS software. The API allows high-level programming languages (e.g., Delphi or Visual Basic) and macro languages (commands with fixed syntax that enable users to vary parameters according to their needs) to execute tasks within a GIS module in a determined order, thereby enabling the automation of the execution of tasks to achieve a certain goal [37].



FIGURE 1: Location of the Lerma-Chapala-Santiago watershed in Mexico.

Notably, four key aspects should be understood by a GIS user in order to effectively implement such modules: First, users should have an overall general understanding of the GIS and its applications, including the formatting of input data, the available analytical tools, and the operational structure of the GIS environment. In addition, users should identify and familiarize themselves with the API of the GIS software and understand macro languages. Knowledge of programming languages for developing API modules within a GIS software is also important, as the results of a particular module are dependent upon the integration of API coding and available analytical functions within the GIS environment. Finally, a user or an analyst must clearly conceptualize the objectives of spatial analysis and programming in order to implement the desired analysis and to create a functional GIS module that provides reliable results.

3. Territorial Framework

The case study area for the verification of the developed module is the Lerma-Chapala-Santiago (LCS) watershed in central Mexico, which encompasses the part of the states of Mexico, Querétaro, Michoacán, Guanajuato, Jalisco, Aguascalientes, Zacatecas, Durango, and Nayarit. The extreme northwestern coordinates are $23^{\circ}26'2.4''$ N and $104^{\circ}18'21.5''$ W, and the extreme southeastern coordinates are $19^{\circ}4'4.8''$ N and $99^{\circ}20'38.4''$ W (Figure 1).

This watershed has an approximate area of $132,916 \text{ km}^2$ [38] that is equivalent to 6.8% of the national territory. Also, this watershed has a total population of 19,495,769

inhabitants and therefore qualifies as the second most populated watershed in the country following the central Valley of Mexico. The population density is 145 inhabitants per km^2 , or three times higher than the national average [39]. Lake Chapala, the largest lake in the country, is found within this watershed and supplies water to a large portion of the metropolitan area of Guadalajara, Jalisco [40]. One of the longest rivers in the country, the Lerma River, also originates in the Toluca Valley (State of Mexico) and empties into Lake Chapala. In addition, the Santiago River originates from Lake Chapala and flows across central Mexico toward its outlet in the Pacific Ocean. These two rivers cross important urban areas (with populations greater than 100,000 inhabitants), including Toluca de Lerdo, Morelia, Uruapan, Zamora de Hidalgo, Querétaro, Celaya, Salamanca, Irapuato, Leon de los Aldama, Guadalajara, Aguascalientes, Tepic, and Zacatecas [38]. Finally, the LCS watershed has a complex and uneven topography, which is one of the determinants of the diverse climate types in the basin.

According to Cotler et al. [41], the upper watershed (Lerma-Chapala) is one of the most socially and economically significant regions of the country; however, this area also forms one of the most environmentally deteriorated regions of the country. The Lerma River is also one of the most notoriously contaminated rivers in Mexico, and the underground water reservoirs of the watershed are largely overexploited [38]. These hydrological and environmental conditions result in large hydrological deficits that create challenges for water management in the region.

4. Materials and Methods

The steps followed to fulfill the objectives of the present study are shown in Figure 2. The method for automating the Köppen–Garcia climate classification (Figure 2(a)) was based on the conceptualization, development, and implementation of a GIS module. As proposed by previous authors, the classic or waterfall model for developing information systems was implemented according to a geomatics approach [42–47]. Overall, this model is composed of five successive stages: analysis of requirements, conceptual design, logical or geomatics design, physical design, and implementation and feedback.

First, in the analysis of the requirements stage, the final desired product was defined. During the conceptual design phase, the subject matter was conceptualized, which served as a framework for the development of the GIS tool. Subsequently, the logical or geomatics design was carried out, and the rationale of the process within the GIS environment was defined. After that, the physical design of the system was performed for the Idrisi Selva GIS using the Object Pascal (Delphi 6.0) programming language. Idrisi Selva was chosen as the GIS because this software is oriented toward performing spatial analyses with raster data. Finally, the Delphi programming language was chosen to enable transparent access to the software's API.

To validate the module for automating climate classification, data from a total of 330 meteorological stations within the LCS watershed meteorological stations, which were published in Garcia [13], were used. In particular, data on climate type and total monthly rainfall and average temperature were inputted into the module. These data were displayed in the raster format as point data representing the monthly values of the climate variables.

The climate classification generated by the automated module was compared with the climate types determined in Garcia [13] using data from the same meteorological stations. Specifically, an agreement analysis was performed using the kappa (K) index [48]. This index generates values between -1 and $+1$. Values closer to $+1$ indicate a higher rate of agreement, while values closer to -1 indicate a higher rate of disagreement [49]. Meanwhile, values near or at zero indicate that the observed agreement is equivalent to what would be expected at random:

$$K = \frac{P_o - \sum_{i=1}^n (p_{i1} \cdot p_{i2})}{1 - \sum_{i=1}^n (p_{i1} \cdot p_{i2})}, \quad (1)$$

where K = kappa index, P_o = proportion of the sum of the diagonal elements of the agreement matrix with respect to the total number of elements, n = the number of categories, i = the number of categories (from 1 to n), p_{i1} = proportion of occurrence of category i for data set 1, and p_{i2} = proportion of occurrence of category i for data set 2.

After the functioning of the module for automating the Köppen–Garcia climate classification method was validated, the climate classifications for the LCS watershed were generated. As the input data also influence the quality of the output data, climate data on rainfall and temperature were

generated using the thin-plate smoothing spline method in the ANUSPLIN package for data interpolation. This method considers variations in longitude, latitude, and altitude as determining factors in climate distribution and goes beyond a simple consideration of the distance between stations, which is a commonly applied criterion in other interpolation methods. Also, the resolution was considered sufficient for clearly delineating the borders of the different climate types; therefore, potential generalizations were avoided by using data with a resolution of greater than 200 m per cell. These data were expressed as interpolated climate layers containing monthly and yearly data for the 1960–2010 period at a cell resolution of 200 m. For the entire LCS watershed, a total of 612 layers per month per variable were generated from a minimum of 1,576 and a maximum of 1,723 weather stations belonging to the National Climatological Database (Base de Datos Climatológica Nacional (CLICOM)), which is administered by the SMN [27].

In addition, to compare climate behavior and average conditions over the complete data period (51 years), the data for the 1960–2010 period (series one) were divided into two periods of 30 years each (Figure 2(b)); this time frame is recommended by the WMO [31] as the minimum time frame necessary for carrying out climate classifications. The 1960–1989 period was denominated as series two, and the 1981–2010 period was denominated as series three. As shown in Figure 2(b), 612 monthly rainfall layers (one for each month for the 1960–2010 period) and 612 average monthly temperature layers (one for each month for the same period) were used as inputs to produce average monthly layers for each time series (1960–2010, 1960–1989, and 1981–2010). As shown in Figure 2(c), the resulting 12 rainfall and 12 temperature layers were used to classify the climate of each time series.

The climate classifications resulting from the procedure outlined in Figure 2(c) were compared (series one was compared to series two and series three) using the Land Change Modeler module in the Idrisi software. Areas with changes in climate type over time were identified in order to analyze climatic transitions (differences in temperature, precipitation, thermal oscillation, and the presence or absence of mid-summer drought in Figure 2(c)). The climate classification layer generated for series one (1960–2010) can be considered as the updated climate map for the LCS watershed.

To analyze the changes between series one (1960–2010) and series two (1960–1989) and between series one (1960–2010) and series three (1981–2010), the following components of the Köppen–Garcia climatic classification were separately considered: nine classes of thermal conditions (warm; cold; very cold; dry arid; dry, very arid; dry, semiarid; semiwarm, warm; semiwarm, temperate; or temperate), two classes of rainfall patterns (summer or winter rains), four classes of thermal oscillation (isothermal, low, extreme, or very extreme), and two classes of drought (the presence or absence of mid-summer drought).

5. Results

The main window of the module for automating the Köppen–Garcia climate classification in the interface of

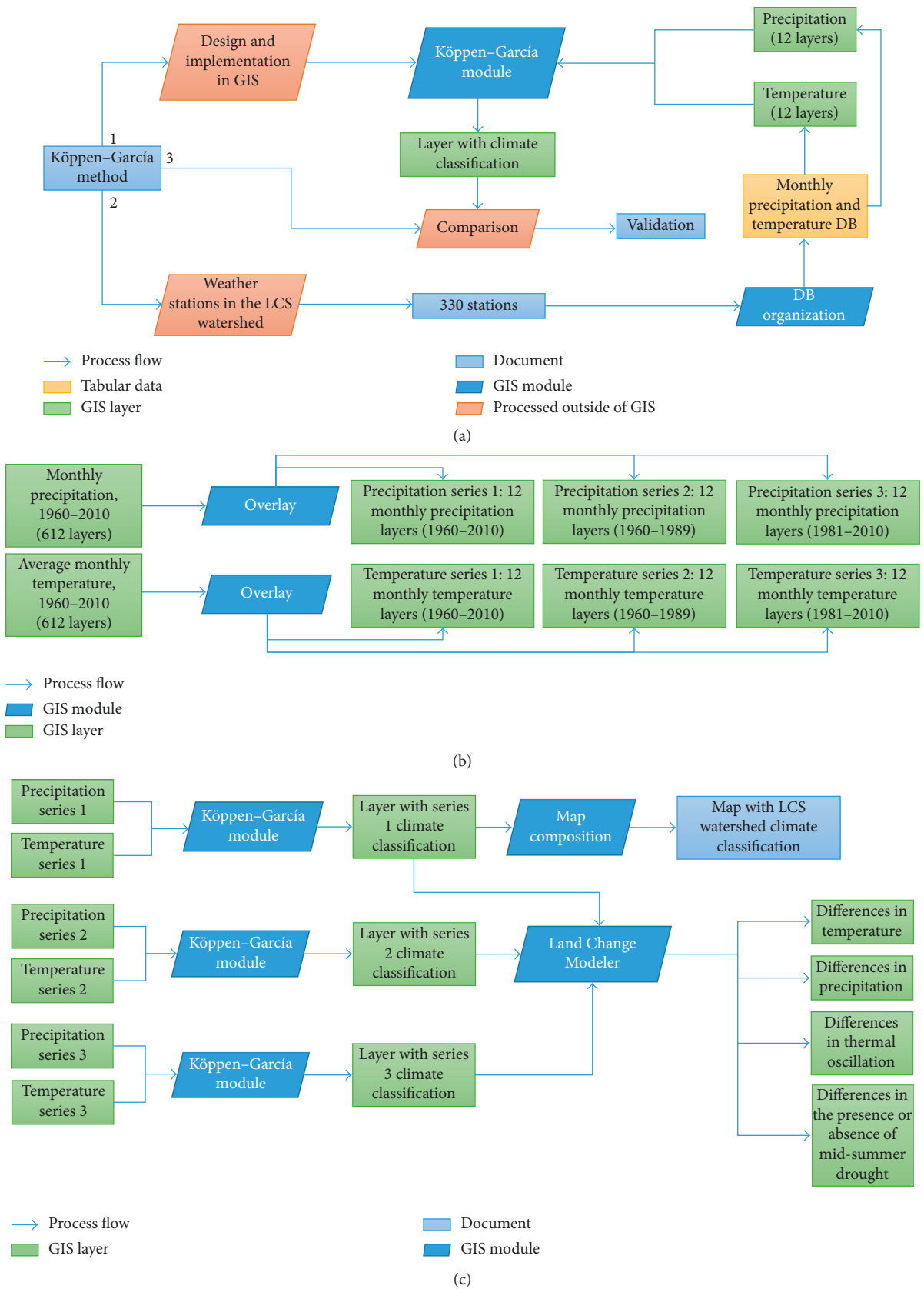


FIGURE 2: Procedures for (a) automating the Köppen-García climate classification method in a GIS module, (b) obtaining three series of monthly rainfall and temperature layers for the Lerma-Chapala-Santiago watershed (1960-2010, 1960-1989, and 1981-2010), and (c) classifying climate per time series.

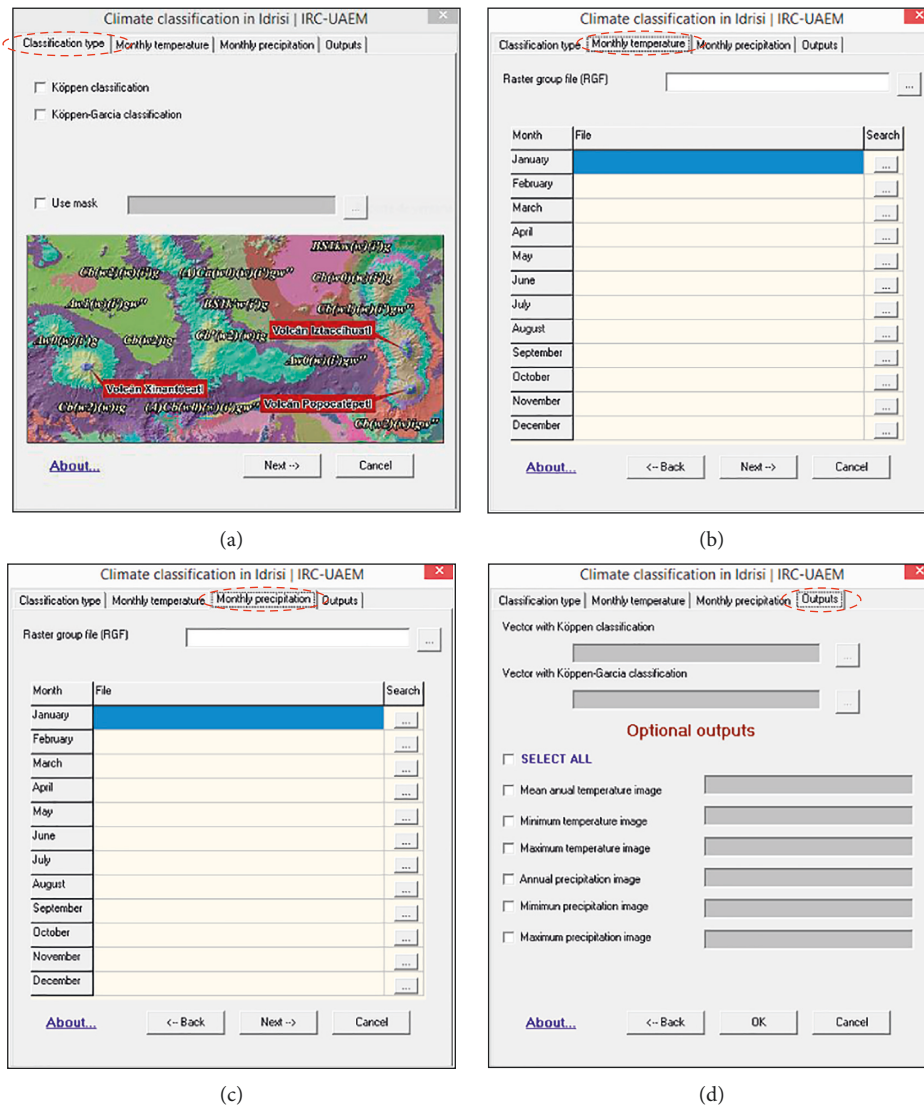


FIGURE 3: Windows for the module automating the Köppen–Garcia climate classification method.

the Idrisi Selva GIS software can be observed in Figure 3. The module consists of four tabs: The first tab allows users to choose between the Köppen and Köppen–Garcia climate classification methods (Figure 3(a)). The second and third tabs prompt the user to input monthly raster layers for temperature and rainfall (Figures 3(b) and 3(c)). Finally, the fourth tab enables users to choose the name and file location of the output file that contains the resulting climate classification for the study zone. Moreover, some additional options enable other data files of interest to be saved, including those on the average, minimum, and maximum temperatures and rainfall throughout the year (Figure 3(d)).

For the basic functioning of the module, a minimum of 12 raster files containing monthly temperature data and 12 raster files containing monthly rainfall data are required (one file for each month of the year). The name of the output file must also be designated. The user interface is simple and easy to use for anyone familiar with GIS. To evaluate the functioning of the module, the kappa index was used to

compare the results of the module with those of the original climate classification of Garcia [13]; a perfect agreement was obtained ($K = 1$) according to Landis and Koch's interpretation of the kappa statistic [49].

Three continuous images based on the time series were generated. These images displayed the monthly rainfall and temperature values for the Lerma-Chapala-Santiago watershed for 1960–2010 (series one), 1981–2010 (series two), and 1960–1989 (series three); all images were derived from interpolated raster layers based on data from meteorological stations. Each series was composed of 12 raster files for rainfall and 12 raster files for temperature. Therefore, the spatial behavior of rainfall and temperature was represented based on their monthly averages per year at a spatial resolution of 200 m per cell. As the geographic position of each meteorological station was taken into account, including the values for altitude, latitude, and longitude, the continuous images expressed the influence of these variables on the spatial distribution of rainfall and temperature within the LCS watershed. In other words, the interpolated values in the resulting raster files are

not necessarily representative of the climatic data recorded at the closest station (which would be the case for an interpolation method solely based on distance) but rather representative of the data recorded at stations with similar altitudinal, latitudinal, and longitudinal characteristics.

One product of this process was the creation of three GIS layers (for each analyzed period) containing the Köppen–Garcia climate classifications. For each series, a vector file linked to an attribute table was also created. The vector file describes the spatial distribution of distinct types of climate within the LCS watershed, while the attribute table stores the qualitative characteristics of the distinct climate types present in the watershed, including the climate symbol, thermal conditions (dry, warm, temperate, or cold), rainfall patterns (summer, winter, or intermediate), other characteristic conditions (cool or warm summer), temperature variations (isothermal, low, extreme, or very extreme), the presence or absence of mid-summer drought, and the annual temperature course (to determine the presence of a Ganges-type temperature regime).

The associated attribute tables allow thematic maps to be created for any of their contained attributes/climate characteristics. This function was used to generate thematic maps for the comparative analysis of changes in temperature conditions, rainfall patterns, temperature variations, and the presence or absence of mid-summer drought between series one (1960–2010) and series two (1960–1989) and between series one (1960–2010) and series three (1981–2010).

Also, to represent climate over the 1960–2010 period, a “Köppen–Garcia climate classification map for the Lerma-Chapala-Santiago watershed, 1960–2010” (Figure 4) was created based on series one (1960–2010). Because of the large dimensions of the watershed and the wide range of climate categories within the area, Figure 4 is presented as a simplified illustration of the original map. The original map contains all the corresponding labels and symbols and can be accessed and printed in larger dimensions.

The map for series one (1960–2010) indicated that the northern and northeastern zones of the watershed presented dry, semiarid climates that corresponded with 36.34% of the total area. Meanwhile, portions of the southern and southeastern watershed presented temperate climates that corresponded with 32.49% of the total area. These regions were located at medium altitudes and contained the sloping hills and mountain peaks that partition the watershed. From the central portion to the western outlet of the watershed, 25.48% of the area was characterized as semiwarm and temperate; in the area immediately surrounding the outlet of the basin toward the coastline, which is characterized by lower altitudes, the climate was warm (5.3% of the total area). The climates with lesser presence in the watershed were found near the partitioning boundaries of the watershed and included the dry arid climates of the northern region (0.23%); the semiwarm, warm climates of the southeastern region (0.13%); and the cold climates at the southern head of the watershed and the summit of the Xinantecatl Volcano, also known as the Nevado de Toluca (0.002%). The temperature variation ranged from null to extreme, with extreme being the most dominant category, while the rainfall pattern predominantly corresponded with

a summer rainfall pattern for nearly the entire watershed (99.9%). The presence of mid-summer drought was only found in the northeastern portion of the watershed (1.8%).

In the comparative analysis of the climate conditions of series one (1960–2010) and series two (1960–1989) (Figure 5 and Table 1), the climate characterizations across 92.8% of the watershed coincided. The remaining 7.2% of the watershed, including northern, central, and eastern areas of the watershed, was classified in series one as dry, semiarid, whereas it was reclassified in series two as dry, arid in the northern zone, as semiwarm, temperate in the central zone, and as temperate in the eastern zone. Notably, in series one, portions of the northern and central watersheds were categorized as temperate, whereas in series two, they were categorized as dry, semiarid in the northern zone and as semiwarm, temperate in the central zone. Only 7.2% of the area differed between series one and two. Overall, the first 30 years of data (series two) were characterized by a hotter and less humid climate in the northern and northwestern portions of the watershed and by a cooler and more humid climate in the southern and southeastern portions in comparison to the complete data period (series one).

In the comparative analysis of the climate conditions of series one (1960–2010) and series three (1981–2010) (Figure 6 and Table 2), the climate characterizations of 93.01% of the watershed coincided. The remaining 6.99% of the watershed showed changes. Notably, regions classified in series one as semiwarm, temperate in the central and northwestern zones of the watershed were classified in series three as dry, semiarid in the central zone and temperate in the northwestern zone; furthermore, areas categorized in series one as temperate in the central and southeastern portions of the watershed were categorized in series three as dry, semiarid in the central zone and semiwarm, temperate in the southeastern zone. Overall, in the last 30 years (series three; 1981–2010), a cooler and more humid climate was found in the central to the northern/northwestern portion of the watershed; from the central to the southeastern portion of the watershed, conditions tended to be warmer and less humid.

The prior comparative analysis reveals that the behavior of rainfall and temperature for the complete data series (series one) (1960–2010) is stable for a large portion of the watershed (for 92.8% of the watershed in series two and for 93% of the watershed in series three) according to the utilized climate classification. However, the climate across the watershed also experienced variations in temperature and rainfall (7.2% for series two and 6.99% for series three) in certain areas. If only the complete 51-year period is considered, such differences might remain imperceptible.

In regard to the rainfall patterns of the LCS watershed, series two (1960–1989) and series three (1981–2010) demonstrated a pattern of summer rainfall across the entire watershed. In series one, 99.9% of the watershed had a summer rainfall pattern; the remaining 0.1% of the area in the northeastern portion of the watershed corresponded with an intermediate rainfall pattern (between summer and winter). Thus, the rainfall patterns of series two and three showed a more homogeneous behavior than temperature patterns.

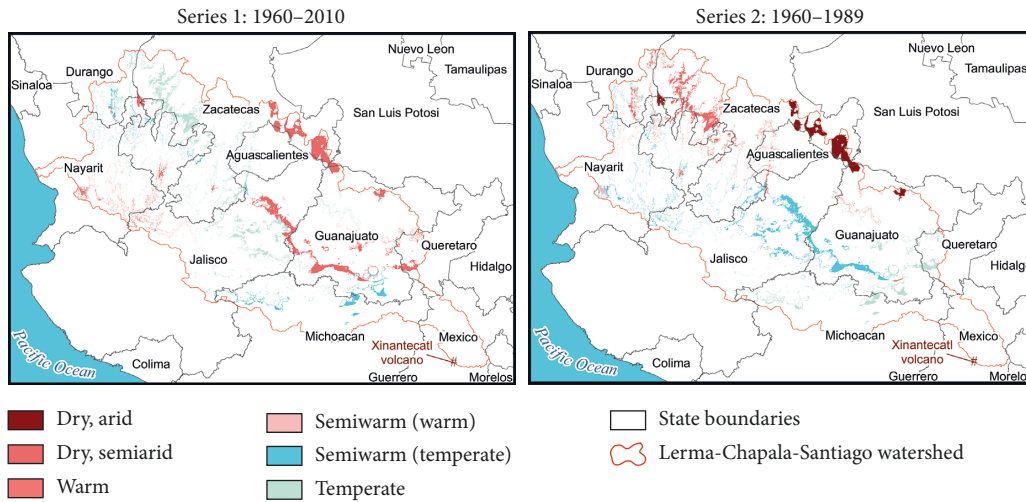


FIGURE 5: Areas of the watershed with changes in temperature conditions between time series one (1960–2010) and time series two (1960–1989).

TABLE 1: Absolute, relative, and proportional areas of the Lerma-Chapala-Santiago watershed with changes in temperature between time series one (1960–2010) and time series two (1960–1989).

No.	Series 1: 1960–2010	Series 2: 1960–1989	Tendency	Surface area with changes		Percentage area of the watershed
				km ²	%	
1	Warm	Semiwarm (temperate)	↓	391.3	4.04	0.292
2	Warm	Semiwarm (warm)	↓	94.7	0.98	0.071
3	Warm	Dry, semiarid	↑*	21.4	0.22	0.016
4	Cold	Temperate	↑	0.8	0.01	0.001
5	Dry, semiarid	Dry, arid	↓*	1,887.2	19.48	1.410
6	Dry, semiarid	Semiwarm (temperate)	↓*	1,642.2	16.95	1.227
7	Dry, semiarid	Temperate	↓*	605.9	6.26	0.453
8	Dry, semiarid	Warm	↓*	40.3	0.42	0.030
9	Semiwarm (warm)	Semiwarm (temperate)	↓	116.3	1.20	0.087
10	Semiwarm (warm)	Warm	↑	2.9	0.03	0.002
11	Semiwarm (temperate)	Temperate	↓	898.5	9.28	0.672
12	Semiwarm (temperate)	Dry, semiarid	↑*	420.2	4.34	0.314
13	Semiwarm (temperate)	Warm	↑	41.4	0.43	0.031
14	Temperate	Dry, semiarid	↑*	1,974.7	20.39	1.476
15	Temperate	Semiwarm (temperate)	↑	1,548.5	15.99	1.157
			Total	9,686.3	100	7.239

*The behavior of rainfall can contribute considerably toward variations in temperature characterization.

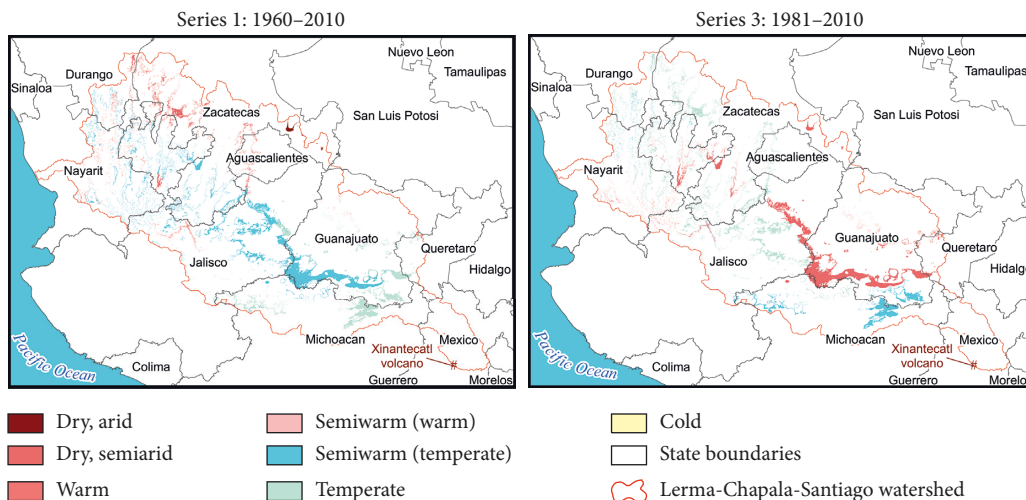


FIGURE 6: Areas of the watershed with changes in temperature conditions between time series one (1960–2010) and time series three (1981–2010).

TABLE 2: Absolute, relative, and proportional areas of the Lerma-Chapala-Santiago watershed with changes in temperature between time series one (1960–2010) and time series three (1981–2010).

No.	Series 1: 1960–2010	Series 3: 1981–2010	Tendency	Surface area with changes		Percentage area of the watershed
				km ²	%	
1	Warm	Dry, semiarid	↑*	155.7	1.665	0.1164
2	Warm	Semiwarm (temperate)	↓	123.4	1.319	0.0922
3	Warm	Semiwarm (warm)	↓	58.3	0.623	0.0436
4	Dry, arid	Dry, semiarid	↓*	85.1	0.909	0.0636
5	Dry, semiarid	Temperate	↓*	922.3	9.861	0.6893
6	Dry, semiarid	Semiwarm (temperate)	↓*	86.2	0.922	0.0644
7	Dry, semiarid	Dry, arid	↑*	4.4	0.047	0.0033
8	Dry, semiarid	Warm	↓*	0.2	0.002	0.0001
9	Semiwarm (warm)	Warm	↑	2.0	0.021	0.0015
10	Semiwarm (warm)	Semiwarm (temperate)	↓	1.3	0.014	0.0010
11	Semiwarm (temperate)	Dry, semiarid	↑*	2,973.1	31.787	2.2219
12	Semiwarm (temperate)	Temperate	↓	2,408.7	25.753	1.8001
13	Semiwarm (temperate)	Semiwarm (warm)	↑	90.9	0.972	0.0679
14	Semiwarm (temperate)	Warm	↑	74.4	0.796	0.0556
15	Temperate	Semiwarm (temperate)	↑	1,461.9	15.630	1.0925
16	Temperate	Dry, semiarid	↑*	904.0	9.665	0.6756
17	Temperate	Cold	↓	1.3	0.014	0.0010
			Total	9,353.1	100	6.99

*The behavior of rainfall can contribute considerably toward variations in temperature characterization.

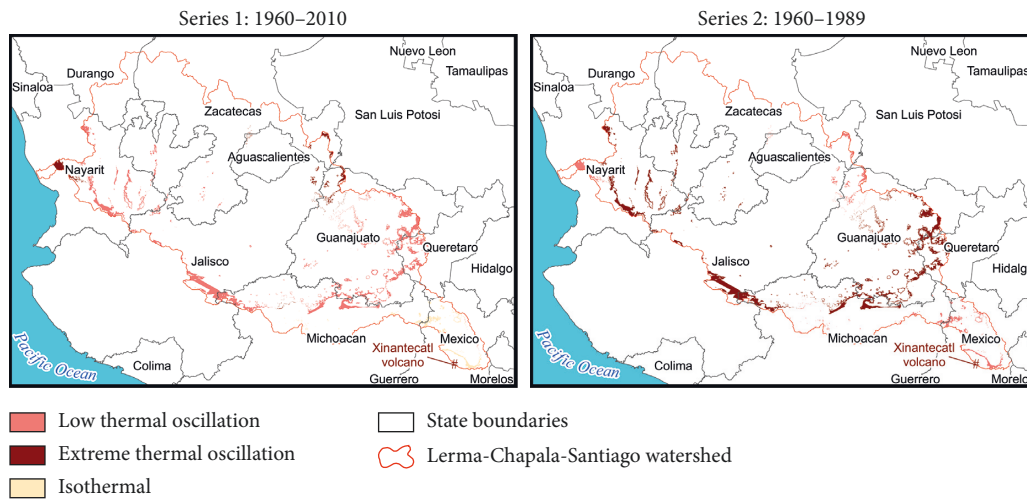


FIGURE 7: Areas of the watershed with changes in thermal oscillation between time series one (1960–2010) and time series two (1960–1989).

The thermal oscillation (the difference between the month with the minimum mean temperature and the month with the maximum mean temperature) between series one (1960–2010) and series two (1960–1989) (Figure 7 and Table 3) was similar for 95.83% of the watershed. The remaining 4.17% of the watershed demonstrated differences in thermal oscillation. Specifically, in series one, extreme thermal oscillation was documented at the eastern and western margins of the watershed; however, in series two, the thermal oscillation was low in these regions. Inversely, in series one, the western, southern, and eastern margins of the watershed showed low thermal oscillation; however, in series two, these areas showed extreme thermal oscillation. Finally, isothermal conditions were present in series one at the headwater of the upper watershed, which is located in the southern portion of the watershed; however, in

series two, low thermal oscillation was found at this site. Overall, in the areas with differences in thermal oscillation between series one and series two, the average difference between maximum and minimum monthly temperatures over the course of the year was greater in series two, especially from the central portion to the southeastern portion of the watershed.

Meanwhile, the thermal oscillation between series one (1960–2010) and series three (1981–2010) (Figure 8 and Table 4) was similar for 94.09% of the watershed. The remaining 5.91% of the watershed demonstrated differences in thermal oscillation. The areas of difference between series one and three are distinct from those between series one and two yet are located in proximity. The southern, eastern, and western margins of the watershed that corresponded with extreme thermal oscillation in series one showed low

TABLE 3: Absolute, relative, and proportional areas of the Lerma-Chapala-Santiago watershed with changes in thermal oscillation between time series one (1960–2010) and time series two (1960–1989).

No.	Series 1: 1960–2010	Series 2: 1960–1989	Tendency	Surface area with changes		Percentage area of the watershed
				km ²	%	
1	Low oscillation	Extreme oscillation	↑	4,391.8	78.7	3.28
2	Low oscillation	Isothermal	↓	13.7	0.2	0.01
3	Extreme oscillation	Low oscillation	↓	560.0	10.0	0.42
4	Isothermal	Low oscillation	↑	616.2	11.0	0.46
			Total	5,581.7	100	4.17

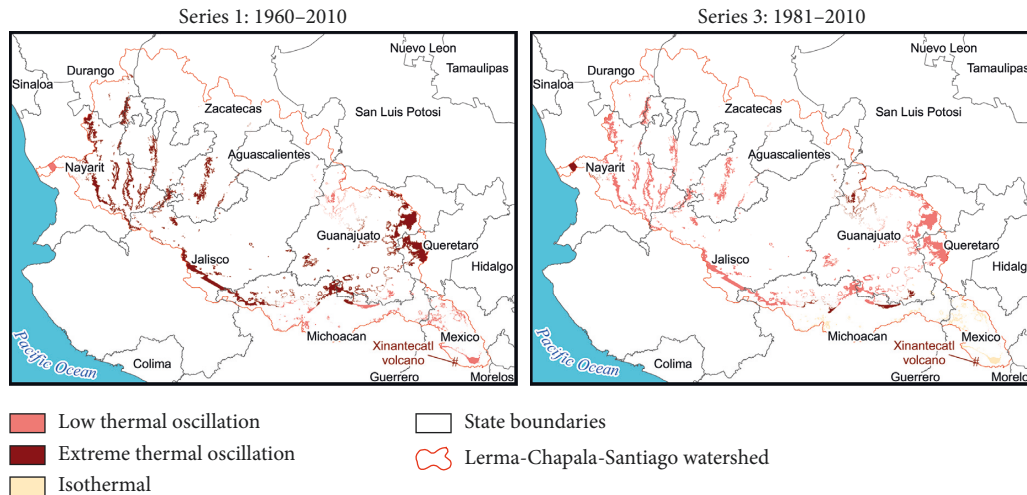


FIGURE 8: Areas of the watershed with changes in thermal oscillation between time series one (1960–2010) and time series three (1981–2010).

TABLE 4: Absolute, relative, and proportional areas of the Lerma-Chapala-Santiago watershed with changes in thermal oscillation between time series one (1960–2010) and time series three (1960–1989).

No.	Series 1: 1960–2010	Series 3: 1981–2010	Tendency	Surface area with changes		Percentage area of the watershed
				km ²	%	
1	Low oscillation	Isothermal	↓	846.5	10.7	0.63
2	Low oscillation	Extreme oscillation	↑	624.2	7.9	0.47
3	Extreme oscillation	Low oscillation	↓	6,421.1	81.2	4.80
4	Isothermal	Low oscillation	↑	11.6	0.1	0.01
			Total	7,903.4	100	5.91

thermal oscillation in series three. The inverse also occurred wherein areas with low thermal oscillation in series one exhibited extreme thermal oscillation in series three. Finally, several areas with low thermal oscillation in the upper watershed in series one were considered isothermal in series three. The zones of distinct thermal oscillation between series one and three (5.91% of the watershed) confirmed a general reduction in the difference between the maximum and the minimum monthly temperatures throughout the year over the last 30 years (1981–2010).

Overall, yearly variations in monthly temperatures in the watershed were largely constant across all time series. The pattern of thermal oscillation differed across 4.2% of the watershed between series one (1960–2010) and series two (1960–1989) and across 5.9% of the watershed between series one (1960–2010) and series three (1981–2010). In the first 30 years, the minimum and maximum monthly temperatures

over the course of one year varied to a greater extent at the upper watershed, whereas the latter 30 years showed the opposite trend: Areas in the upper watershed showed a reduction in the oscillation between average minimum and maximum monthly temperatures.

The final climate classification parameter that was compared among the three time series was the presence or absence of mid-summer drought. Series two (1960–1989) and series three (1981–2010) coincided in 98.9% of the watershed area, whereas the areas of difference represented 1.1% of the watershed. The areas of difference were located in several areas along the northeastern margin and headwaters of the watershed (at Xinantecatl Volcano) (Figures 9 and 10; Tables 5 and 6). In the comparison of series one (1960–2010) and series two, areas experiencing mid-summer drought in series one were marked as areas without mid-summer drought in series two. Inversely, areas in series one that

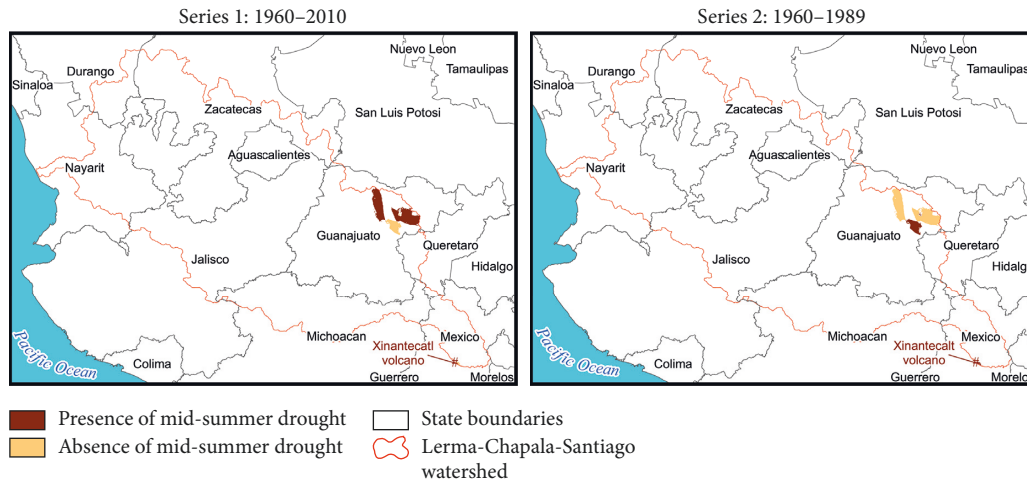


FIGURE 9: Areas of the watershed with changes in the presence or absence of mid-summer drought between time series one (1960–2010) and time series two (1960–1989).

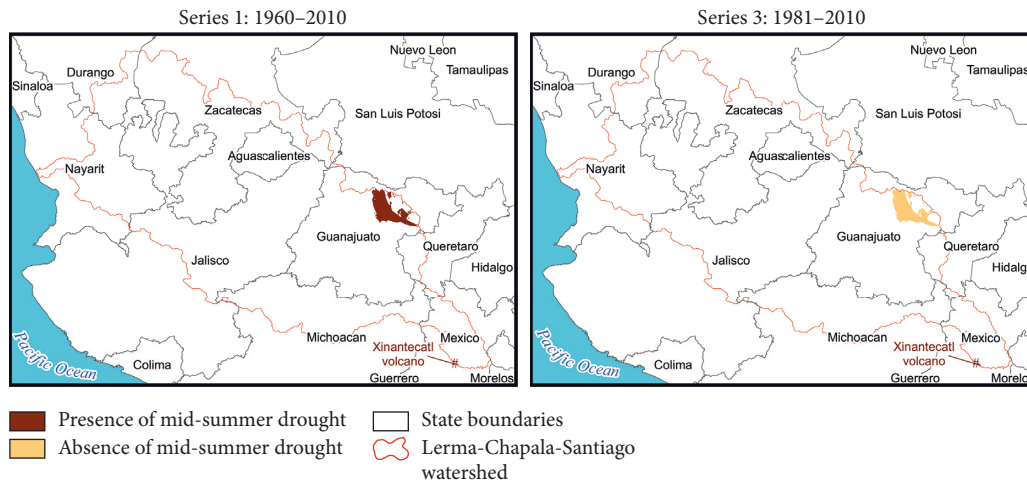


FIGURE 10: Areas of the watershed with changes in the presence or absence of mid-summer drought between time series one (1960–2010) and time series three (1981–2010).

TABLE 5: Absolute, relative, and proportional areas of the Lerma-Chapala-Santiago watershed with changes in the presence or absence of mid-summer drought between time series one (1960–2010) and time series two (1960–1989).

No.	Series 1: 1960–2010	Series 2: 1960–1989	Tendency	Surface area with changes		Percentage area of the watershed
				km ²	%	
1	Presence	Absence	↓	1,191.9	80.4	0.9
2	Absence	Presence	↑	291.1	19.6	0.2
			Total	1,483	100	1.1

TABLE 6: Absolute, relative, and proportional areas of the Lerma-Chapala-Santiago watershed with changes in the presence or absence of mid-summer drought between time series one (1960–2010) and time series three (1960–1989).

No.	Series 1: 1960–2010	Series 3: 1981–2010	Tendency	Surface area with changes		Percentage area of the watershed
				km ²	%	
1	Presence	Absence	↓	1,500.0	98.9	1.12
2	Absence	Presence	↑	16.3	1.1	0.01
			Total	1,516.3	100	1.13

lacked mid-summer drought showed this phenomenon in series two and three. In other words, 1.1% of the watershed demonstrated the occurrence of mid-summer drought in the complete data series (1960–2010), although this meteorological phenomenon was not detected during the shorter periods (series two and three). In addition, differences are evident in the volcano region: Series one indicates an absence of mid-summer drought, although the other two series confirm its presence.

The high rate of coincidence in the area (98.9%) of series one (1960–2010) with respect to series two (1960–1989) and series three (1981–2010) in regard to the presence or absence of a mid-summer drought indicates that the monthly rainfall distribution is steady during the rainy season (in the summer) for a large portion of the watershed. The majority of the watershed does not experience mid-summer drought, with the exception of a small portion of the northeastern watershed.

6. Conclusions

In the present study, an automated Köppen–Garcia climate classification of the Lerma-Chapala-Santiago watershed was performed in a GIS using rainfall and temperature layers. The proposed module for automating this classification method demonstrated a perfect degree of agreement in comparison to the results of a previous nonautomated study. Therefore, the proposed module was successful in achieving its objectives. This module can be used to classify the climate of any region at the raster cell level in a GIS using available point data on rainfall and temperature.

Traditionally, methods for climate classification have relied on extending point data from meteorological stations to nearby areas regardless of differences in altitude or other conditions. Therefore, the aim of the present research was to create a more accurate display of climate across a continuous area. Interpolated layers of monthly rainfall and temperature were inputted in a GIS. The values for each cell of the resulting raster layer were not solely based on the rainfall and temperature values recorded at nearby meteorological stations (according to the distance) but also based on the values recorded at stations with shared characteristics like latitude, longitude, and elevation. In this sense, each cell within the resulting raster layer was evaluated as if it contained a meteorological station. The accuracy of this classification method was validated using the kappa index. Upon comparing the results of the developed GIS module to those of a previous non-automated classification, the resulting value of the kappa statistic ($K = 1$) confirmed the perfect agreement of the classification methods.

This module has several important applications: First, this module can spatially express point data sets from meteorological stations and can therefore facilitate the use of large quantities of climate data generated by meteorological stations throughout Mexico. Second, this module can generate climate maps for different regions of the study of varying territorial extension. Also, this module can be used to easily update climate maps as the steps are

automated. Finally, studies spanning or comparing different time frames of the same region can use this module to identify tendencies in spatial and temporal climate patterns or even to compare future climate scenarios by utilizing data sets from the IPCC. Therefore, this module can quickly and easily generate Köppen–Garcia climate classification maps for all regions of Mexico at any cell resolution or spatial extension desired by the user, whether for a microwatershed or the entire country.

The Köppen–Garcia climate classification map for the Lerma-Chapala-Santiago watershed based on climate data from 1960 to 2010 represents one of the most current and detailed maps for the region up to the present date. The proposed module also facilitated the comparative analysis of climate behavior in this watershed during 1960–2010 with that of two shorter periods, 1960–1989 and 1981–2010. Overall, the monthly behavior of temperature and rainfall was constant over the course of the 51 analyzed years. The climate characterization of at least 92% of the watershed area coincided in temperature, extreme temperature, and rainfall and in the presence or absence of mid-summer drought. For the remaining portions of the watershed, the noted climate variations should be considered during the development of management plans or during decision-making, especially in regard to issues that are potentially dependent upon or influenced by climate. Finally, the Idrisi Resource Center of Mexico is building a website to distribute the new climate classification module presented herein, which is available at the following link: <http://idrisi.uaemex.mx/index.php/distribucion/gratis/clasificacion-climatica-koppen-garcia>.

Conflicts of Interest

The authors declare that there are no conflicts of interest.

Acknowledgments

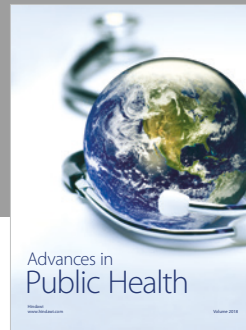
This study was carried out with the financial support provided by CONACYT under research projects 248498 and 248553 and the UAEM/Quebec Grant 4192/2016E.

References

- [1] W. Bach, *Man's Impact on Climate*, Vol. 10, Elsevier, New York, NY, USA, 2012.
- [2] N. Scafetta and A. Mazzearella, "The Arctic and Antarctic Sea-ice area index records versus measured and modeled temperature data," *Advances in Meteorology*, vol. 2015, Article ID 481834, 8 pages, 2015..
- [3] V. R. Barros, C. B. Field, D. J. Dokken et al., *Climate Change 2014: Impacts, Adaptation, and Vulnerability-Part B: Regional Aspects-Contribution of Working Group II to the Fifth Assessment Report of the Intergovernmental Panel on Climate Change*, Cambridge University Press, Cambridge, UK, 2014.
- [4] R. Di Cristo, A. Mazzearella, and R. Viola, "An analysis of heat index over Naples (Southern Italy) in the context of European heat wave of 2003," *Natural Hazards*, vol. 40, no. 2, pp. 373–379, 2007.
- [5] J. Tonnetto and A. Carbonneau, "A multicriteria climatic classification system for grape-growing regions worldwide,"

- Agricultural and Forest Meteorology*, vol. 124, no. 1-2, pp. 81-97, 2004.
- [6] D. H. White, G. A. Lubulwa, K. Menz, H. Zuo, W. Wint, and J. Slingenbergh, "Agro-climatic classification systems for estimating the global distribution of livestock numbers and commodities," *Environment International*, vol. 27, no. 2-3, pp. 181-187, 2001.
- [7] E. Baltas, "Spatial distribution of climatic indices in northern Greece," *Meteorological Applications*, vol. 14, no. 1, pp. 69-78, 2007.
- [8] J. H. Eum, D. Scherer, U. Fenrenbach, and J. H. Woo, "Development of an urban landcover classification scheme suitable for representing climatic conditions in a densely built-up Asian megacity," *Landscape and Urban Planning*, vol. 103, no. 3-4, pp. 362-371, 2011.
- [9] O. Rakoto-Joseph, F. Garde, M. David, L. Adelaar, and Z. A. Randriamanantany, "Development of climatic zones and passive solar design in Madagascar," *Energy Conversion and Management*, vol. 50, no. 4, pp. 1004-1010, 2009.
- [10] S. M. Kumar, S. Mahapatra, and S. K. Atreya, "Development of bio-climatic zones in north-east India," *Energy and Buildings*, vol. 39, no. 12, pp. 1250-1257, 2007.
- [11] L. Tang and F. Hossain, "Investigating the similarity of satellite rainfall error metrics as a function of Köppen climate classification," *Atmospheric Research*, vol. 104-105, pp. 182-192, 2012.
- [12] E. García, *Modificaciones al sistema de clasificación climática de Köppen (para adaptarlo a las condiciones de la república mexicana)*, Talleres de offset Larjos, Tacubaya, México, 1987.
- [13] E. García, *Modificaciones al Régimen de Clasificación Climática de Köppen*, Instituto de Geografía-UNAM, Ciudad de México, México, 2004.
- [14] S. N. Sánchez and L. R. Garduño, "Algunas consideraciones acerca de los sistemas de clasificación climática," *Revista Electrónica Contacto*, vol. 68, pp. 5-10, 2008, <http://www.izt.uam.mx/newpage/contactos/index.php/Numeros-anteriores.html>.
- [15] Observatorio de Cambio Climático de Yucatán, *Atlas de escenarios de Cambio Climático en la Península de Yucatán. Tipos de climas. Secretaría de Desarrollo Urbano y Medio Ambiente del Gobierno del Estado de Yucatán*, 2010, <http://www.cambioclimatico.yucatan.gob.mx/escenarios-cambio-climatico/index.php>.
- [16] L. C. Hernández, *Análisis del comportamiento de la temperatura y precipitación mediante climogramas y tendencias en la zona central de Veracruz. Tesis inédita de la licenciatura en Ciencias Atmosféricas de la Facultad de Instrumentación Electrónica y Ciencias Atmosféricas*, Universidad Veracruzana, Xalapa, Mexico, 2012.
- [17] Gobierno del Estado de Durango, *Ordenamiento ecológico del Estado de Durango*, Secretaría de Recursos Naturales y Medio Ambiente del Gobierno del Estado de Durango, Durango, Mexico, pp. 40-51, 2011.
- [18] R. A. Velázquez, R. Martínez, M. C. G. Luis, and M. Fátima, "Caracterización climática para la región de Bahía de Banderas mediante el sistema de Köppen, modificado por García, y técnicas de Sistemas de Información Geográfica," *Investigaciones Geográficas*, no. 79, pp. 7-19, 2012.
- [19] Sistema Nacional de Vigilancia Epidemiológica Fitosanitaria, *Atlas Multimedia*, Medio ambiente. Clima. Secretaría de Agricultura, Ganadería, Desarrollo Rural, Pesca y Alimentación del Gobierno Federal, Mexico, 2013, <http://portal.sinavef.gob.mx/atlasMultimedia/atlasFitosanitario.html>.
- [20] Instituto Nacional de Estadística y Geografía, *Recursos Naturales. Climatología. Información Climática*, 2014, <http://www.inegi.org.mx/geo/contenidos/recnat/clima/infoclimatica.aspx>.
- [21] F. Fuentes and A. Víctor, *Clasificación climática de acuerdo a Köppen-García*, Hoja de cálculo. Laboratorio de Investigaciones en Arquitectura Bioclimática, Ciudad de México, Mexico, 2000, http://arq-bioclimatica.com/index.php?option=com_phocadownload&view=.
- [22] G. Sparovek, L. Van, J. Quirijin, and D. N. Durval, "Computer assisted Koeppen climate classification: a case study for Brazil," *International Journal of Climatology*, vol. 27, no. 2, pp. 257-266, 2007.
- [23] L. Liu, B. Timbal, J. Mo, and H. Fairweather, "A GIS-based climate change adaptation strategy tool," *International Journal of Climate Change Strategies and Management*, vol. 3, no. 2, pp. 140-155, 2010.
- [24] R. Ahmed, "Polygonal map generation with realistic climate zoning," Project Report, School of Computer Science and Communication, KTH Royal Institute of Technology, Stockholm, Sweden, 2012.
- [25] Environmental Systems Research Institute, *Koppen-Geiger Observed and Predicted Climate Shifts*, International User Community, Environmental Systems Research Institute, Redlands, CA, USA, 2012, <http://www.arcgis.com/home/item.html?id=0b9f1f90f4f745daacbc35599609b59a>.
- [26] F. Rubel and M. Kottek, "Observed and projected climate shifts 1901-2100 depicted by world maps of the Köppen-Geiger climate classification," *Meteorologische Zeitschrift*, vol. 19, no. 2, pp. 135-141, 2010.
- [27] A. P. Cuervo-Robayo, O. Téllez-Valdés, M. A. Gómez-Albores, C. S. Venegas-Barrera, J. Manjarrez, and E. Martínez-Meyer, "An update of high-resolution monthly climate surfaces for Mexico," *International Journal of Climatology*, vol. 34, no. 7, pp. 2427-2437, 2014.
- [28] K. L. Ebi, L. O. Mearns, and B. Nyenzi, "Weather and climate: changing human exposure," in *Climate Change and Human Health*, World health Organization, Geneva, Switzerland, 2003.
- [29] Intergovernmental Panel on Climate Change, *Climate Change 2001: The Scientific Basis. Contribution of Working Group I to the Third Assessment Report of the Intergovernmental Panel on Climate Change*, Cambridge University Press, Cambridge, UK, 2001.
- [30] R. Barry, A. Eileen, and H. McKim, *Essentials of the Earth's Climate System*, Cambridge University Press, New York, NY, USA, 2014.
- [31] World Meteorological Organization WMO, *International Glossary of Hydrology*, World Meteorological Organization, Geneva, Switzerland, 2012.
- [32] M. Sanderson, "The classification of climates from Pythagoras to Köppen," *Bulletin of the American Meteorological Society*, vol. 80, no. 4, pp. 669-673, 1999.
- [33] M. Kottek, J. Grieser, C. Beck, B. Rudolf, and F. Rubel, "World map of the Köppen-Geiger climate classification updated," *Meteorologische Zeitschrift*, vol. 15, no. 3, pp. 259-263, 2006.
- [34] J. R. Eastman, *Manual Version 17.01, Fourier Analysis*, Clark Labs, Clark University, Worcester, MA, USA, 2012.
- [35] E. P. Boer, K. M. de Beurs, and A. D. Hartkamp, "Kriging and thin plate splines for mapping climate variables," *International Journal of Applied Earth Observation and Geo-information*, vol. 3, no. 2, pp. 146-154, 2001.
- [36] A. Mazzarella and G. Tranfaglia, "Fractal characterization of geophysical measuring networks and its implication for an optimal location of additional stations: an application to a rain-gauge network," *Theoretical and Applied Climatology*, vol. 65, no. 3-4, pp. 157-163, 2000.

- [37] Clark Labs, *IDRISI Applications Programming Interface User's Guide. Versión 2.0*, Clark Labs, Clark University, Worcester, MA, USA, 2003.
- [38] CONAGUA, *Lerma-Chapala Basin Case Study Mexico: A Fruitful Sustainable Experience*, 1–28, 2012, <http://www.conagua.gob.mx/CONAGUA07/Contenido/Documentos/LermaChapalaBasinCase.pdf>.
- [39] Instituto Nacional de Estadística y Geografía, *Censos y conteos de población y vivienda 2010*, 2014, <http://www.inegi.org.mx/est/contenidos/proyectos/ccpv/>.
- [40] Comisión Estatal del Agua de Jalisco, *Cuencas, Lago de Chapala*, Gobierno del Estado de Jalisco, Jalisco, México, 2017, <http://www.ceajalisco.gob.mx/>.
- [41] H. Cotler, S. Gutierrez, C. Enriquez, and A. Garrido, “The evaluation of soil erosion off-sites effects in large basins: the study case of Lerma-Chapala watershed, Mexico,” *Revista Sociedade and Natureza*, vol. 1, no. 1, pp. 941–952, 2005.
- [42] Environmental Systems Research Institute, *ArcGIS 9. Getting Started with ArcGIS*, Environmental Systems Research Institute, Redlands, CA, USA, 2007.
- [43] M. D. C. Heras Sánchez, J. A. Ochoa Granillo, C. Watts Thorp, J. A. Saiz Hernández, R. G. Hazas Izquierdo, and M. Á. Gómez Albores, “Modelación tridimensional-temporal-temática de parámetros hidroclimáticos distribuidos en la cuenca del Río San Miguel,” *Computación y Sistemas*, vol. 17, no. 3, pp. 423–434, 2013.
- [44] R. Franco-Plata, L. R. Manzano-Solís, M. A. Gómez-Albores, J. I. Juan-Pérez, N. B. Pineda-Jaimes, and A. Martínez-Carrillo, “Using a GIS tool to map the spatial distribution of population for 2010 in the State of Mexico, Mexico,” *Journal of Geographic Information System*, vol. 4, no. 1, pp. 1–11, 2012.
- [45] R. Franco-Plata, C. Miranda-Vázquez, H. Solares-Hernández, L. R. Manzano-Solís, K. M. Bâ, and J. L. Expósito-Castillo, “Implementing into GIS a tool to automate the calculation of physiographic parameters of river basins,” *Open Journal of Modern Hydrology*, vol. 3, no. 2, pp. 67–74, 2013.
- [46] V. Demir and O. Kisi, “Flood hazard mapping by using geographic information system and hydraulic model: Mert River, Samsun, Turkey,” *Advances in Meteorology*, vol. 2016, Article ID 4891015, 9 pages, 2016.
- [47] R. F. Tomlinson, *Thinking about GIS: Geographic Information System Planning for Managers*, ESRI Inc., Redlands, CA, USA, 2007.
- [48] M. I. Sameen and B. Pradhan, “A two-stage optimization strategy for fuzzy object-based analysis using airborne LiDAR and high-resolution orthophotos for urban road extraction,” *Journal of Sensors*, vol. 2017, Article ID 6431519, 17 pages, 2017.
- [49] J. L. Fleiss, J. Cohen, and B. S. Everitt, “Large sample standard errors of kappa and weighted kappa,” *Psychological Bulletin*, vol. 72, no. 5, pp. 323–327, 1969.



Hindawi

Submit your manuscripts at
www.hindawi.com

